Original Article

Effect of body mass index (BMI) on image contrast in the hepatobiliary phase of Gd-EOB-DTPA-enhanced-MRI and the feasibility of the application of half-dose Gd-EOB-DTPA to hepatobiliary phase imaging in patients with a BMI less than 24: a comparative study

Rongsheng Chen[#], Yunfeng Lu[#], Zhibo Xiao, Zhiwei Zhang, Fajin Lv, Furong Lv

Department of Radiology, The First Affiliated Hospital of Chongqing Medical University, Chongqing, China

Contributions: (I) Conception and design: R Chen, Furong Lv; (II) Administrative support: Furong Lv; (III) Provision of study materials or patients: R Chen, Y Lu; (IV) Collection and assembly of data: R Chen, Y Lu; (V) Data analysis and interpretation: R Chen, Y Lu, Z Xiao, Z Zhang, Furong Lv; (VI) Manuscript writing: All authors; (VII) Final approval of manuscript: All authors.

[#]These authors contributed equally to this work.

Correspondence to: Furong Lv, MD. Department of Radiology, The First Affiliated Hospital of Chongqing Medical University, No. 1, Youyi Road, Yuanjiagang, Yuzhong District, Chongqing 400042, China. Email: cql@hospital.cqmu.edu.cn.

Background: Gadolinium-ethoxybenzyl-diethylenetriamine-pentaacetic acid (Gd-EOB-DTPA)-enhanced magnetic resonance imaging (MRI) can detect more lesions through the image contrast of hepatobiliary phase. Body mass index (BMI) reflects the composition ratio of human tissue, which is an influencing factor of magnetic resonance image contrast. Meanwhile, Gd-EOB-DTPA is recommended to use the minimum dose when the diagnosis demands could be met. The aim of this paper was to investigate the effect of BMI on hepatobiliary phase image contrast and explore the feasibility of using low-dose Gd-EOB-DTPA to obtain good hepatobiliary phase image contrast in patients with normal and lean BMI.

Methods: Eighty-two patients who had previously undergone Gd-EOB-DTPA-enhanced MRI (0.025 mmol/kg) were collected and divided into group A (BMI <24 kg/m^2) and group B (BMI ≥24 kg/m^2) according to Chinese BMI standards. Liver-to-portal vein contrast ratio (LPC20) and liver-to-spleen contrast ratio (LSC20) in hepatobiliary phase (20 min after injection) were calculated. Thirty patients with a BMI <24 kg/m^2 who were about to receive Gd-EOB-DTPA-enhanced MRI were randomly divided into group C (0.0125 mmol/kg) and group D (0.025 mmol/kg). Image acquisition was performed at 10, 15, and 20 min after injection. LPC10, LPC15, LPC20 and LSC10, LSC15, LSC20 in corresponding phases were calculated.

Results: In retrospective grouping study, compared with group B, group A's LPC20 was significantly higher [2.63 (2.42–3.00) *vs.* 2.22 (1.97–2.67); P<0.01]. In prospective grouping study, there were no differences in LPC15, LSC15, LPC20 and LSC20 between group C and group D. Intragroup comparison in each group showed that LPC15 (group C: 2.67±0.33; group D: 2.61±0.21) and LPC20 (group C: 2.74±0.37; group D: 2.72±0.27) were higher than LPC10 (group C: 2.19±0.18; group D: 1.94±0.17) (all P<0.01), while there were no changes between LPC15 and LPC20.

Conclusions: Under conventional dose, hepatobiliary phase image contrast in patients with a BMI <24 was higher, which was mainly manifested in the high LPC. For patients with a BMI <24 kg/m^2, using a half conventional dose (0.0125 mmol/kg), good hepatobiliary phase image contrast can still be obtained at 15–20 min after administration.

Keywords: Gadolinium-ethoxybenzyl-diethylenetriamine-pentaacetic acid (Gd-EOB-DTPA); hepatobiliary phase; body mass index (BMI); low dose

Submitted May 11, 2023. Accepted for publication Jul 07, 2023. Published online Jul 21, 2023.
doi: 10.21037/qims-23-653
View this article at: https://dx.doi.org/10.21037/qims-23-653

Introduction

Gadolinium-ethoxybenzyl-diethylenetriamine-pentaacetic acid (Gd-EOB-DTPA) is a hepatocyte-specific gadolinium-based contrast agent (GBCA) that is widely used in liver-enhanced magnetic resonance imaging (MRI). Gd-EOB-DTPA-enhanced MRI can obtain both dynamic enhancement and unique hepatobiliary images, the hepatobiliary images could provide additional diagnostic information for hepatic hemangioma, metastases, hepatocellular carcinomas, focal nodular hyperplasia (FNH) and other disease. So compared to other extracellular contrast agent-enhanced MRI, Gd-EOB-DTPA-enhanced MRI can detect more lesions and make qualitative diagnoses for some of them (1-5). Therefore, high-quality hepatobiliary images are key to the success of Gd-EOB-DTPA-enhanced MRI. Image contrast, as an important indicator of image quality in the hepatobiliary phase, plays a crucial role in improving the detection of lesions (6-8). Previous studies have shown that liver function, contrast media dose, and scan parameters are influencing factors of hepatobiliary phase image contrast (9,10). However, most of these studies have ignored the influence of human tissue composition ratio on the image contrast of hepatobiliary phase and in terms of clinical application of Gd-EOB-DTPA, it also has been noted that even after controlling for the above influencing factors, the image contrast of the hepatobiliary phase in patients still lacks good consistency (11).

The composition ratio of human tissue is an important influencing factor of all magnetic resonance image contrast (12,13), and body mass index (BMI), as one of the commonly used indices to measure the degree of fat and thinness of the human body and whether it is healthy, reflects the composition ratio of human tissue to a certain extent (14-16), However, the effect of BMI on hepatobiliary phase image contrast in Gd-EOB-DTPA-enhanced MRI has not been reported. At the same time, studies have shown that GBCAs may induce adverse reactions such as nephrogenic systemic fibrosis NSF when injected intravenously (17-19). Some scholars have speculated that the excessive application of GBCAs may also be a risk factor for the above adverse reactions (20). And GBCAs including Gd-EOB-DTPA are recommended to use the minimum dose when the diagnostic demands could be met (21). But in the clinical applications, a dosage of 0.025 mmol/kg body weight Gd-EOB-DTPA is used in all patients for hepatobiliary phase imaging, regardless of whether the image contrast of hepatobiliary phase were way above diagnostic requirements.

Therefore, the present study retrospectively analyzed the hepatobiliary phase image contrast in Gd-EOB-DTP-enhanced MRI in patients with different BMIs and explored the feasibility of using low-dose (0.0125 mmol/kg) Gd-EOB-DTPA to obtain good image contrast in the hepatobiliary phase in patients with normal and lean BMIs. We present this article in accordance with the GRRAS reporting checklist (available at https://qims.amegroups.com/article/view/10.21037/qims-23-653/rc).

Methods

Study design

This study was conducted in two parts: a retrospective grouping study and a prospective grouping study. The retrospective grouping study analyzed historical data, while the prospective grouping study focused on collecting new data over a specified period.

Participants

Retrospective grouping study of regular doses

In this part, patients who had previously undergone Gd-EOB-DTPA-enhanced MRI scans from January 2019 to January 2021 at The First Affiliated Hospital of Chongqing Medical University were collected. The exclusion criteria were as follows: (I) cases in which there were no reports of biochemical indices of liver and kidney function within 3 days before the examination or the test indicator value was not within the normal value range of the laboratory that issued the report [Child-Pugh score and glomerular

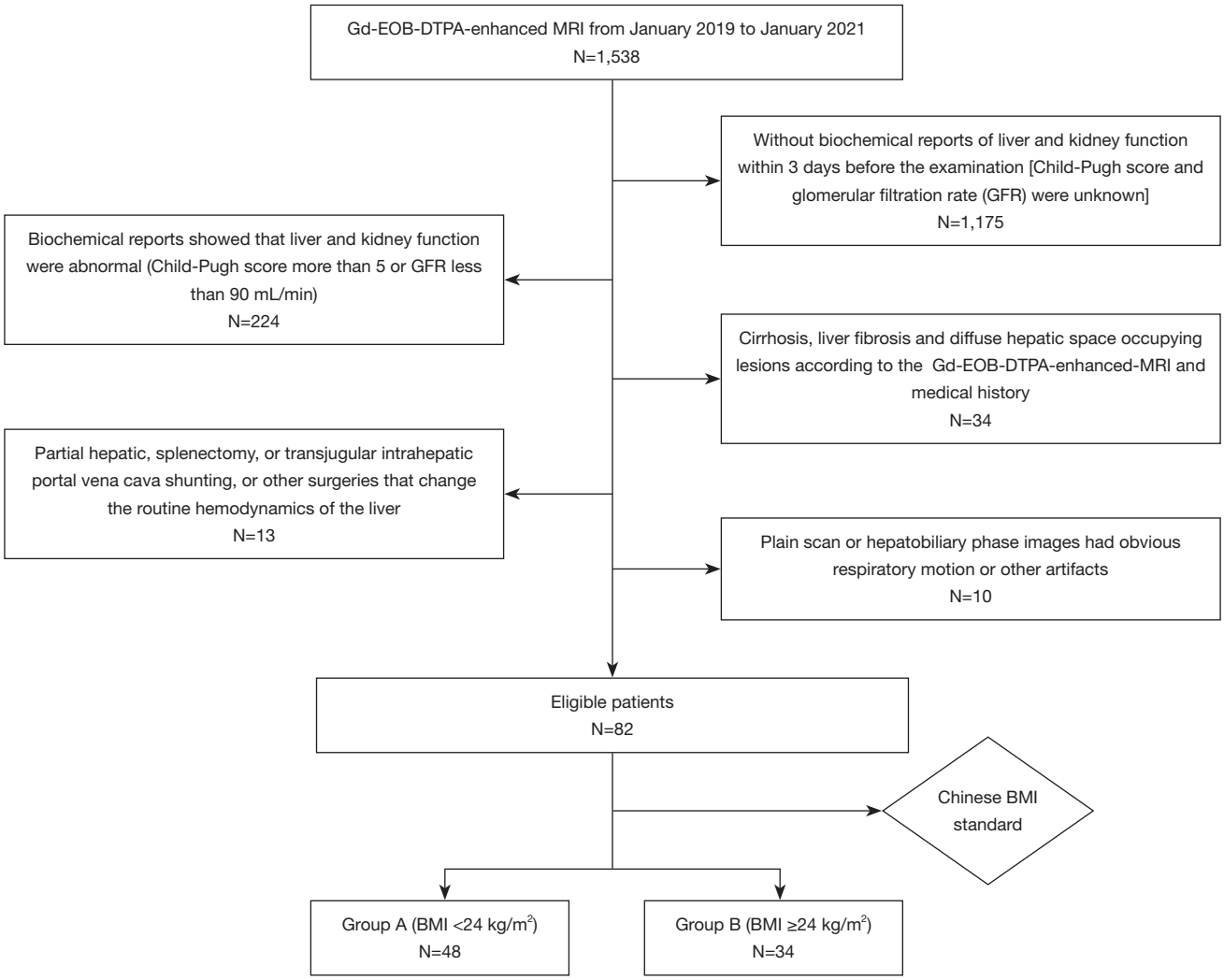

Figure 1 Flow chart of the selection process for narrowing down the target patients in retrospective grouping study of regular doses. Gd-EOB-DTPA, gadolinium-ethoxybenzyl-diethylenetriamine-pentaacetic acid; MRI, magnetic resonance imaging; BMI, body mass index.

filtration rate (GFR) were unknown, Child-Pugh score more than 5 or GFR less than 90 mL/min] were excluded to rule out the impact of different liver and kidney function on study results; (II) plain scan or hepatobiliary phase images had obvious respiratory motion or other artifacts, which were not conducive to observation and measurement; (III) patients were diagnosed with abnormal liver iron deposition, cirrhosis, liver fibrosis and diffuse hepatic space occupying lesions according to the Gd-EOB-DTPA-enhanced-MRI and medical history; and (IV) patients who had undergone chemo-radiotherapy and transcatheter arterial chemoembolization, partial hepatic, splenectomy, or transjugular intrahepatic portal vena cava shunting, or other surgeries that change the routine hemodynamics of the liver. Eighty-two patients were included and divided into two groups: group A (normal and lean group: BMI <24 kg/m^2, n=48) and group B (overweight and obese group: BMI ≥24 kg/m^2, n=34) according to the Chinese BMI standard (22) in this part (*Figure 1*). The patients' corresponding BMI values were calculated from the recorded heights and weights.

Prospective grouping study of different dose

In this part, Patients with a BMI <24 kg/m^2 who were about to undergo Gd-EOB-DTPA-enhanced MRI from December 2021 to April 2022 at The First Affiliated Hospital of Chongqing Medical University were collected. The inclusion criteria were as follows: (I) patients

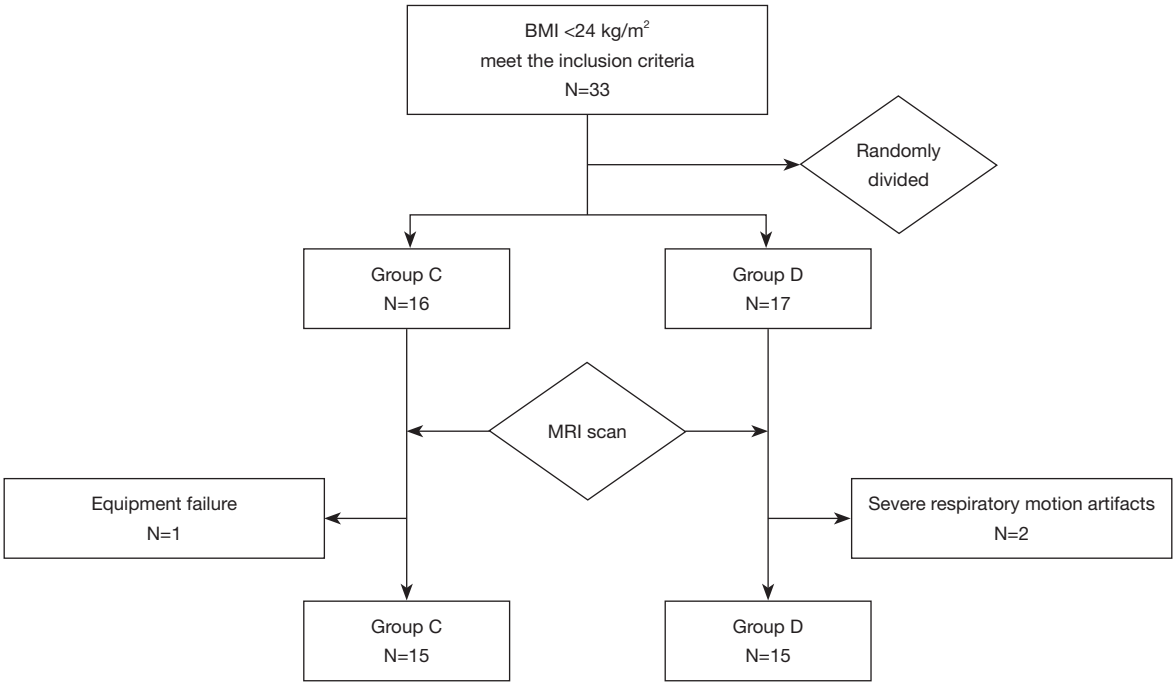

Figure 2 Flow chart of the selection process for narrowing down the target patients in prospective grouping study of different dose. Group C: low-dose group; Group D: conventional-dose group. BMI, body mass index; MRI, magnetic resonance imaging.

who could cooperate with the examination and had no contraindications related to MRI examination and a single breath-holding time of more than 20 s; (II) the biochemical index report of liver and kidney function in the 3 days before the examination showed that the liver and kidney function were normal (Child-Pugh score was 5 and GFR more than 90 mL/min); (III) patients who had undergone chemo-radiotherapy and transcatheter arterial chemoembolization, partial hepatic, splenectomy, or transjugular intrahepatic portal vena cava shunting, or other surgeries that change the routine hemodynamics of the liver; and (IV) patients were diagnosed with abnormal liver iron deposition, cirrhosis, liver fibrosis and diffuse hepatic space occupying lesions according to medical history. Thirty-three patients who met the inclusion criteria were collected and randomly divided into two groups: group C (low-dose group, n=16) and group D (conventional-dose group, n=17) for MRI scan. The exclusion criteria were as follows: (I) failure to complete the examination on time due to unexpected circumstances (such as equipment failure, intolerance to the inspection process, etc.); (II) Gd-EOB-DTPA-enhanced MRI image artifacts were serious; and (III) patients were diagnosed with abnormal liver iron deposition, cirrhosis, liver fibrosis and diffuse hepatic space occupying lesions according to Gd-EOB-DTPA-enhanced MRI. One case in group C was excluded due to sudden equipment failure during the scanning process, two cases in group D were excluded due to severe respiratory motion artifacts, and the remaining 30 patients were included in this part. Each group included 15 cases, respectively (*Figure 2*).

The study was conducted in accordance with the Declaration of Helsinki (as revised in 2013). The study was approved by the Ethics Committee of The First Affiliated Hospital of Chongqing Medical University and informed consent was taken from all the patients.

MR examination and contrast medium injection protocols

Both retrospective and prospective studies utilized the same MRI scanners and imaging parameters. All patients were scanned in the feet first-supine position, the Signa HDxt 3.0 Tesla MRI system (GE Medical Systems, Waukesha, WI, United States) and 8-channel phased array abdominal coil (GE Medical Systems, Waukesha, WI, United States) were utilized. Unenhanced and hepatobiliary phase imaging were all performed at the identical scan range by using fat-suppressed three-dimensional (3D) T1-weighted

Table 1 Comprehensive list of delayed time

Phase	Plain scan	Contrast	10 min after injection	15 min after injection	20 min after injection
Retrospective grouping study of regular doses	Group A	0.025 mmol/kg	–	–	Group A
	Group B	0.025 mmol/kg	–	–	Group B
Prospective grouping study of different dose	Group C	0.0125 mmol/kg	Group C	Group C	Group C
	Group D	0.025 mmol/kg	Group D	Group D	Group D

Group A: normal and lean group (BMI <24 kg/m^2); Group B: overweight and obese group (BMI ≥24 kg/m^2); Group C: low-dose group; Group D: conventional-dose group. BMI, body mass index.

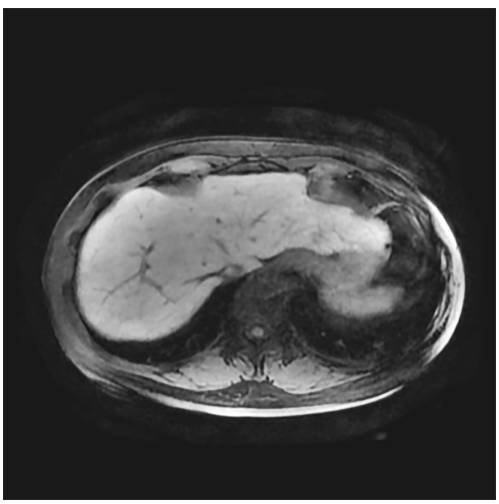

Figure 3 Flow-related enhancement effect at the hepatic vein into the inferior vena cava, which made the signal measurement error large.

gradient echo pulse sequence (liver acquisition with volume acceleration, lava) sequence. Lava imaging parameters were as follows: repetition time (TR) 3.2 ms, echo time (TE) 1.4 ms, field of view (FOV) 38 cm, flip angle 15°, matrix size 288×224, layer thickness 4 mm, frequency direction LR, zero-fill interpolation processing (ZIP) 512, ZIP2 and array coil spatial sensitivity encoding (ASSET) were turned on, the acceleration factor selection was 2. Upon completion of the plain scan, in the retrospective grouping study of regular doses, a bolus of Gd-EOB-DTPA was administered at a dosage of 0.025 mmol/kg body weight through the dorsal hand vein or median cubital vein for all patients (both group A and B), followed by a 20 mL physiological saline solution flushing tube. The hepatobiliary phase was only scanned at 20 min after the injection. In the prospective grouping study of different dose, A bolus of Gd-EOB-DTPA was administered at a dosage of 0.0125 mmol/kg body weight in group C and 0.025 mmol/kg body weight in group D, all followed by a 20 mL physiological saline solution flushing tube. Both groups were image-acquired at 10, 15, and 20 min after the injection of contrast medium (see *Table 1*).

Image analysis

According to the requirements of the liver imaging reporting and data system (LI-RADS) v2018 CT/MRI Manual for the image contrast of Gd-EOB-DTPA-enhanced MRI hepatobiliary phase (Hepatic parenchyma is hyperintense to the hepatic blood vessels and spleen), liver-to-portal vein contrast ratio (LPC) and liver-to-spleen contrast ratio (LSC) were used to quantitatively assess the image contrast of the hepatobiliary phase in this study. The portal vein signal was taken as a reference for the hepatic blood vessels owing to the follows: the trunk and branches of hepatic arteries were too small and their signals decayed rapidly after they reached the peak in the arterial phase, which meant that their signals were difficult to observe and measure in the hepatobiliary phase. The hepatic vein signal was mainly affected by the contrast content in the hepatic portal vein and flow-related enhancement effect could be observed in it (*Figure 3*), which meant that a large signal measurement error interfered with the study results. In contrast, the hepatic portal vein continued to strengthen for a long time after administration and decayed slowly, and its trunk and branches were large; thus, the signal was easy to perceive and measure.

For the measurement of the liver, spleen, portal vein signals and noise, all images were transmitted to the GE AW4.6 post-processing workstation and performed in each phase (plain scan, 10 min, 15 min, 20 min) and each group by drawing region of interest (ROI). For measurement of hepatic parenchymal signal (SL, SL10, SL15, SL20), the

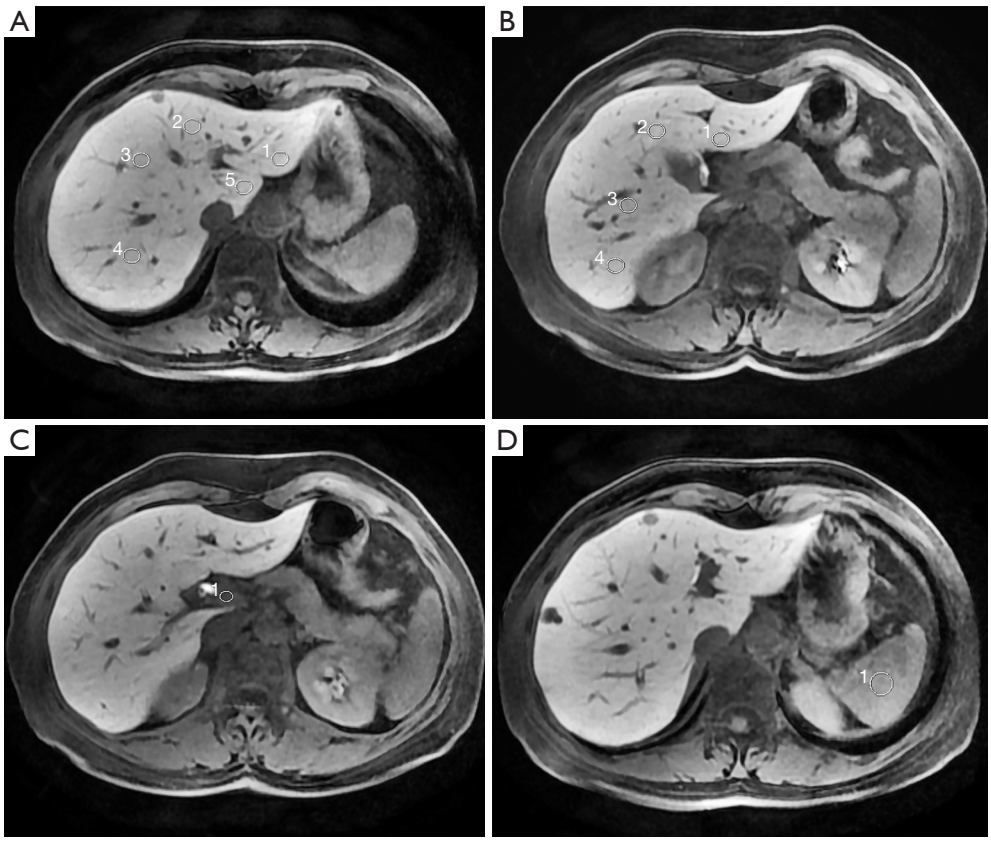

Figure 4 The location of ROIs as measured in each organ. (A,B) The location of the ROIs as measured in the liver [circles 1–5 (A) and circles 1–4 (B)]; (C) the location of the ROIs as measured in the portal vein (circle 1); (D) the location of the ROIs as measured in the spleen (circle 1). ROIs, regions of interest.

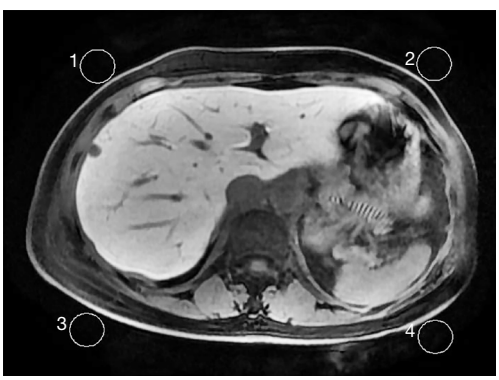

Figure 5 The location of the ROIs as measured in the noise (circles 1–4). ROIs, regions of interest.

ROIs were placed at the central region of the maximum layer of each liver segment (according to the Couinaud method) and then the average value of these segments was calculated, ROI areas: 0.8–1.2 cm^2; for measurement of portal vein (SP, SP10, SP15 and SP20) and splenic parenchymal signal (SS, SS10, SS15, SS20), the ROIs were placed at the central region of the maximum layer of the main portal vein and spleen, respectively, ROI areas: 0.3–0.4 cm^2 for the portal vein and 2.0–2.8 cm^2 for the spleen (*Figure 4*); for measurement of the background noise (SN, SN10, SN15 and SN20), 4 ROIs were placed next to the abdominal wall at the maximum layer of liver and then the average value of standard deviation of the 4 regions was calculated, ROI areas: 3–4 cm^2 (*Figure 5*). When measuring,

Table 2 Patient demographics table of retrospective grouping study of regular doses

Patient characteristic	Group A	Group B
No. of participants (male/female)	48 (25/23)	34 (19/15)
Age (years), mean ± SD [range]	50.40±12.54 [23–82]	50.24±12.42 [24–86]
BMI (kg/m^2), mean ± SD [range]	21.44±1.74 [18.07–23.88]	26.84±1.78 [24.07–30.12]
Hepatic hemangiomas, n	15	12
Hepatic cyst, n	8	7
Hepatic metastases, n	12	10
Fatty liver, n	3	12
Hepatocellular carcinoma, n	2	3
Focal nodular hyperplasia, n	2	2

Group A: normal and lean group (BMI <24 kg/m^2); Group B: overweight and obese group (BMI ≥24 kg/m^2). BMI, body mass index; SD, standard deviation.

ROIs must be placed in a uniform signal place by avoiding other non-targeted tissues and must be measured at the same size and in the same anatomical position when measuring the same data on each phase image. Based on the above conditions, the ROI areas would be as large as possible. All data were measured once by two radiologists independently, each with more than 5 years of experience in liver MRI, and then the average value was calculated. The following signal intensity ratios in each phases (plain scan, 10 min, 15 min, 20 min) were calculated from the measured data, LPC, LPC10, LPC15, LPC20 (ratio of hepatic parenchymal signal to portal vein signal; LPCx = SLx/SPx, where x was the delay time), LSC, LSC10, LSC15, LSC20 (ratio of hepatic parenchymal signal to splenic parenchymal signal: LSCx = SLx/SSx, where x was the delay time), the following relative tissue enhancement were also calculated, LE10, LE15, LE20 (ratio of hepatic parenchymal signal in the corresponding phases to hepatic parenchymal signal in the plain scan: Lex = SLx/SL, where x was the delay time). PE10, PE15, PE20 (ratio of portal vein signal in the corresponding phases to portal vein signal in the plain scan: PEx = SPx/SP, where x was the delay time), SE10, SE15, SE20 (ratio of splenic parenchymal signal in the corresponding phases to splenic parenchymal signal in the plain scan, SEx = SSx/SS, where x was the delay time), the signal-to-noise ratio and contrast-to-noise ratio were also calculated, SNRL,SNRL10, SNRL15, SNR20 (hepatic parenchymal signal to noise ratio: SNRLx = SLx/SNx, where x was the delay time), SNRP, SNRP10, SNRP15, SNRP20 (portal vein signal to noise ratio: SNRPx = SPx/SNx, where x was the delay time), SNRS, SNRS10, SNRS15, SNRS20 (splenic parenchymal signal to noise ratio: SNRSx = SSx/SNx, where x was the delay time), CNRLP, CNRLP10, CNRLP15, CNRLP20 (absolute value of the difference between hepatic parenchymal signal and portal vein signal to noise ratio: CNRLPx = |SLx – SPx|/SNx, where x was the delay time), CNRLS, CNRLS10, CNRLS15, CNRLS20 (absolute value of the difference between hepatic parenchymal signal and splenic parenchymal signal to noise ratio: CNRLSx = |SLx – SSx|/SNx, where x was the delay time).

Statistical analysis

Software of SPSS26 (Chicago, IL, United States) was used to analyze the statistical data in the retrospective and the prospective grouping study. Shapiro-Wilk test were used for the normality of the indices, an independent sample *t*-test was used to compare the indices between the groups when they satisfied a normal distribution, while those with a non-normal distribution were compared using the Mann-Whitney *U* test. In the prospective grouping study of different dose, One-way variance analysis was used for intragroup comparisons of the indices when the variance was even, while the Welch test was used when the variance was uneven. Moreover, the Bonferroni method was used for intragroup pairwise comparisons when the variances were even, and the Tamhane T2 method was used when the variances were uneven. All the statistical tests were used two-sided test, P<0.05 was considered statistically significant.

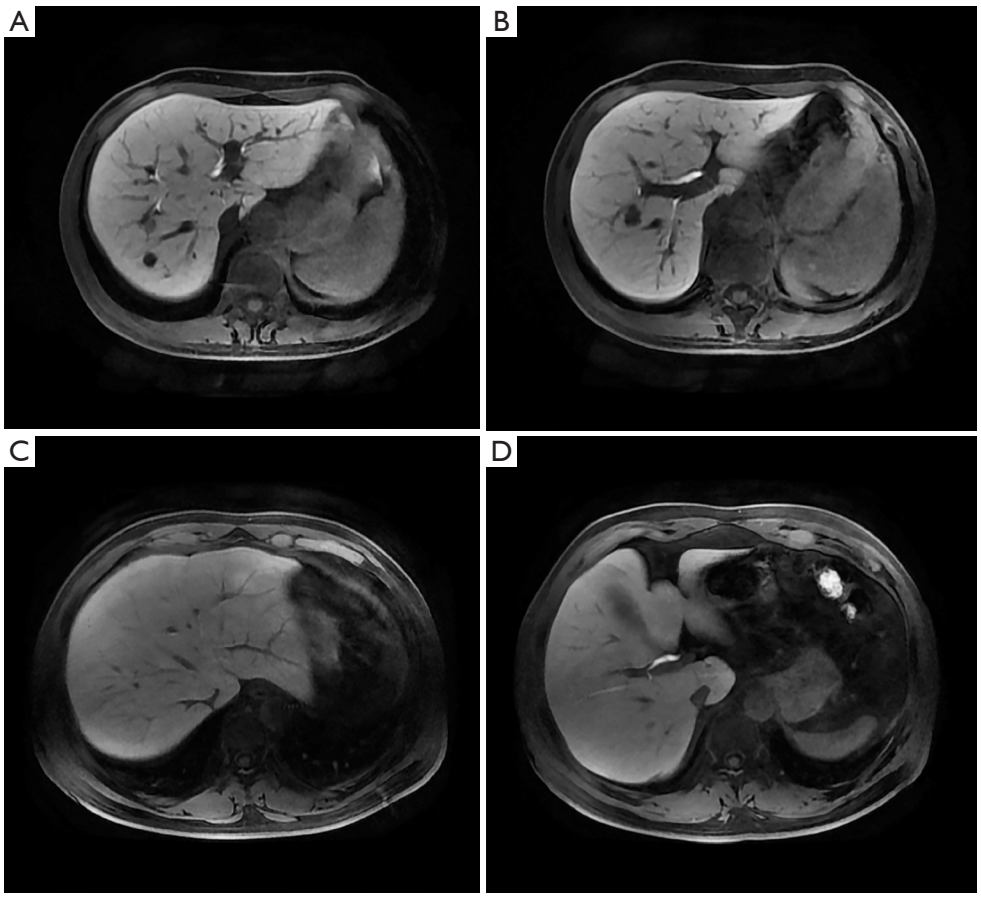

Figure 6 Retrospective grouping study of regular doses. (A,B) Hepatobiliary phase images of a patients with a BMI =20.54 kg/m^2 in group A, the LPC20 and the LSC20 were 2.84 and 1.21, respectively; (C,D) hepatobiliary phase images of a patients with a BMI =29.78 kg/m^2 in group B. The LPC20 and the LSC20 were 2.18 and 1.15, respectively. BMI, body mass index; LPC20, the contrast between liver and portal vein, ratio of hepatic parenchymal signal to portal vein signal in 20 min after injection; LSC20, the contrast between liver and spleen, ratio of hepatic parenchymal signal to splenic parenchymal signal in 20 min after injection.

Results

Results of the retrospective grouping study of regular doses

The demographics of the 82 patients in the retrospective grouping study of regular doses were listed in *Table 2*. Quantitative analysis showed that the liver-to-portal vein contrast ratio of plain scan and 20 min after injection (LPC and LPC20) in group A were significantly higher than that in group B (P<0.01). But there were no statistical differences in the liver-to-spleen contrast ratio (LSC and LSC20) (P>0.05) (*Figures 6*,*7*, *Table 3*).

Results of the grouping study on different doses administered

The demographics of the 30 patients in the prospective grouping study of different dose were listed in *Table 4*. SNR and CNR analyses showed that no significant difference in the SNR of each tissue in plain scan and other phases between group C and D. But the contrast-to-noise ratio of liver-to-portal vein in 10 min after injection (CNRLP10) in group C was higher than that in group D (P<0.05) (*Figure 8*, *Table 5*).

Quantitative comparative analysis indicated that there

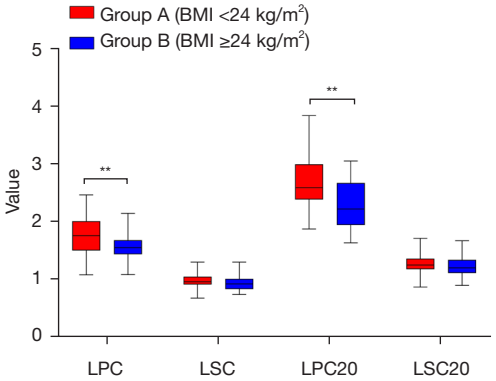

Figure 7 Retrospective grouping studies comparing data between groups A and B. **, P<0.01. LPC and LPC20, the contrast between liver and portal vein, ratio of hepatic parenchymal signal to portal vein signal in the plain scan and 20 min after injection; LSC and LSC20, the contrast between liver and spleen, ratio of hepatic parenchymal signal to splenic parenchymal signal in the plain scan and 20 min after injection; BMI, body mass index.

was no significant difference in liver-to-portal vein contrast ratio and liver-to-spleen contrast ratio (LPC and LSC) between group C and D in the plain scan. But in the 10 min phase after administration, the liver-to-portal vein contrast ratio (LPC10) in group C was higher than that in group D, while the relative tissue enhancement of liver, portal vein and spleen (LE10, PE10, and SE10) of group D were higher than those in group C (P<0.01). And there was no statistically significant difference observed in liver-to-spleen ration (LSC10) (P>0.05). At the 15 and 20 min phases after administration, the relative tissue enhancement of each organ (LE15, PE15, SE15, LE20, PE20, and SE20) in group D were higher than those in group C (P<0.01), while there were no significant changes in the liver-to-portal vein contrast ratio and liver-to-spleen contrast ratio (LPC15, LSC15, LPC20, and LSC20) between the two groups (P>0.05) (see *Figures 9,10*, *Table 6*).

Intragroup comparative analysis showed that the

Table 3 Retrospective grouping studies comparing data between groups A and B

Index	LPC	LSC	LPC20	LSC20
Group A (BMI <24 kg/m²)	1.76±0.31	0.96±0.10	2.63 (2.42–3.00)*	1.27±0.17
Group B (BMI ≥24 kg/m²)	1.58±0.24	0.94±0.13	2.22 (1.97–2.67)*	1.23±0.17
t/*Z* value	2.884	0.841	–3.370*	1.272
P value	<0.01	0.403	<0.01*	0.207

*, a significant difference at a P value <0.05 was observed using the Mann-Whitney *U* test. Indices were presented as mean ± standard deviation when the samples followed the normal distribution and median (lower quartile – upper quartile) when the samples did not follow the normal distribution. LPC and LPC20, the contrast between liver and portal vein, ratio of hepatic parenchymal signal to portal vein signal in the plain scan and 20 min after injection; LSC and LSC20, the contrast between liver and spleen, ratio of hepatic parenchymal signal to splenic parenchymal signal in the plain scan and 20 min after injection; BMI, body mass index.

Table 4 Patient demographics table of prospective grouping study of different dose

Patient characteristic	Group C	Group D
No. of participants (male/female)	15 (6/9)	15 (3/12)
Age (years), mean ± SD [range]	48.27±11.93 [30–64]	57.53±13.22 [33–79]
BMI (kg/m²), mean ± SD [range]	21.36±1.40 [19.10–23.50]	22.18±1.29 [19.82–23.88]
Hepatic hemangiomas, n	4	2
Hepatic cyst, n	6	10
Hepatic metastases, n	3	3
Fatty liver, n	1	1
Hepatocellular carcinoma, n	1	0

Group C: low-dose group; Group D: conventional-dose group. BMI, body mass index; SD, standard deviation.

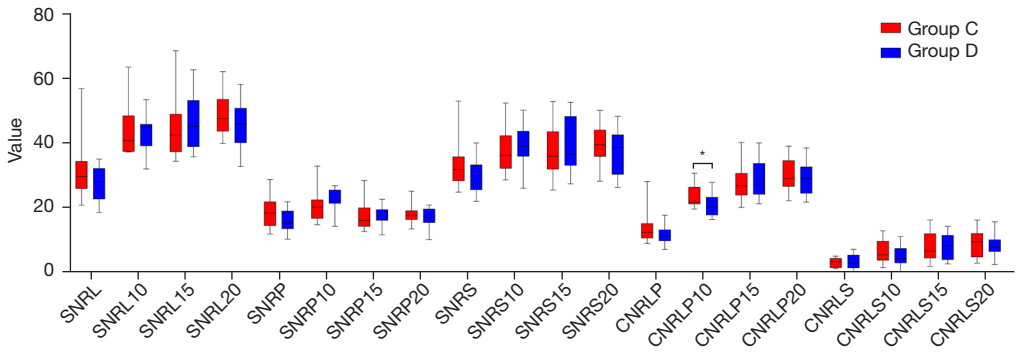

Figure 8 Intergroup comparison of SNR and CNR in different dose groups. *, P<0.05. Group C: low-dose group; Group D: conventional-dose group. SNRL and SNRL 10/15/20, the signal to noise ratio of liver, hepatic parenchymal signal to noise ratio in plain scan and corresponding phases; SNRP and SNRP 10/15/20, the signal to noise ratio of portal vein, portal vein signal to noise ratio in plain scan and corresponding phases; SNRS and SNRS 10/15/20, the signal to noise ratio of spleen, splenic parenchymal signal to noise ratio in plain scan and corresponding phases; CNRLP and CNRLP 10/15/20, the contrast to noise ratio of liver-portal vein, absolute value of the difference between hepatic parenchymal signal and portal vein signal to noise ratio in plain scan and corresponding phases; CNRLS and CNRLS 10/15/20, the contrast to noise ratio of liver-spleen, absolute value of the difference between hepatic parenchymal signal and splenic parenchymal signal to noise ratio in plain scan and corresponding phases; SNR, signal to noise ratio; CNR, contrast to noise ratio.

Table 5 Intergroup comparison of SNR and CNR in different dose groups

Index	Group C	Group D	*t*/*Z* value	P value
SNRL	32.27±8.82	27.71±5.31	1.713	0.098
SNRL10	44.20±7.89	43.69±5.26	0.211	0.835
SNRL15	45.44±9.49	46.55±7.74	−0.351	0.728
SNRL20	48.77±9.49	46.21±7.74	1.003	0.325
SNRP	18.77±5.05	16.11±3.46	1.679	0.104
SNRP10	20.40±4.63	22.72±3.38	1.563	0.129
SNRP15	17.28±4.25	17.83±2.65	−0.429	0.671
SNRP20	18.05±3.04	17.10±2.87	0.882	0.385
SNRS	33.98±7.12	30.00±5.23	1.744	0.092
SNRS10	37.76±6.28	39.67±5.99	−0.852	0.401
SNRS15	37.46±7.61	38.79±8.12	0.463	0.647
SNRS20	39.66±5.83	38.01±7.12	0.693	0.494
CNRLP	13.50±4.64	11.60±2.76	1.365	0.183
CNRLP10	23.80±3.85	20.97±3.21	2.186	0.037
CNRLP15	28.17±6.25	28.72±5.51	−0.257	0.799
CNRLP20	30.72±5.32	29.11±5.24	0.834	0.411
CNRLS	3.03±1.40	3.30±2.30	−0.389	0.7
CNRLS10	6.44±3.52	5.14±3.44	1.019	0.317
CNRLS15	7.99±4.85	8.11±3.75	−0.08	0.937
CNRLS20	9.12±4.32	8.53±3.57	0.401	0.691

Indices were presented as mean ± standard deviation when the samples followed the normal distribution. Group C: low-dose group; Group D: conventional-dose group. SNR, signal to noise ratio; CNR, contrast to noise ratio; SNRL, the signal to noise ratio of liver, hepatic parenchymal signal to noise ratio in plain scan and corresponding phases; SNRP, the signal to noise ratio of portal vein, portal vein signal to noise ratio in plain scan and corresponding phases; SNRS, the signal to noise ratio of spleen, splenic parenchymal signal to noise ratio in plain scan and corresponding phases; CNRLP, the contrast to noise ratio of liver-portal vein, absolute value of the difference between hepatic parenchymal signal and portal vein signal to noise ratio in plain scan and corresponding phases; CNRLS, the contrast to noise ratio of liver-spleen, absolute value of the difference between hepatic parenchymal signal and splenic parenchymal signal to noise ratio in plain scan and corresponding phases.

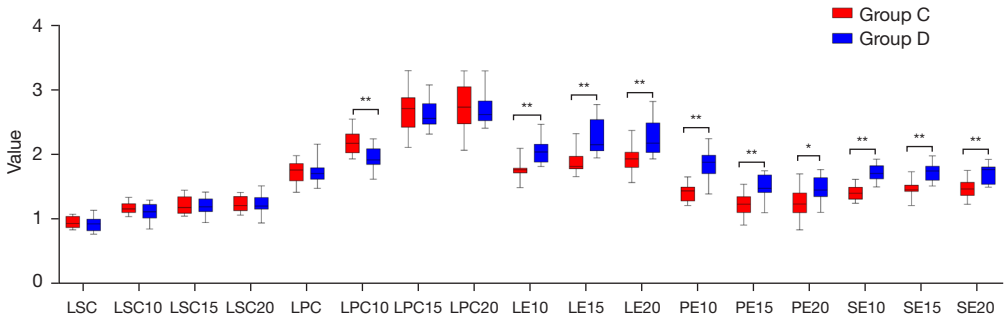

Figure 9 Intergroup comparison of the indices in different dose groups. *, P<0.05; **, P<0.01. Group C: low-dose group; Group D: conventional-dose group. LSC and LSC10/15/20, the contrast between liver and spleen, ratio of hepatic parenchymal signal to splenic parenchymal signal in the plain scan and corresponding phases; LPC and LPC10/15/20, the contrast between liver and portal vein, ratio of hepatic parenchymal signal to portal vein signal in the plain scan and corresponding phases; LE10/15/20, the relative tissue enhancement of liver, ratio of hepatic parenchymal signal in the corresponding phases to hepatic parenchymal signal in the plain scan; PE10/15/20, the relative tissue enhancement of portal vein, ratio of portal vein signal in the corresponding phases to portal vein signal in the plain scan; SE10/15/20, the relative tissue enhancement of spleen, ratio of splenic parenchymal signal in the corresponding phases to splenic parenchymal signal in the plain scan.

differences between the liver-to-portal vein contrast ration of each phase (LPC10, LPC15 and LPC20) were statistically significant in the two groups (P<0.01), and the pairwise comparison showed that the LPC15 and LPC20 were higher than the LPC10 (P<0.01), but the difference between the LPC15 and LPC20 was not significant (P>0.05). There were no significant differences between the liver-to-spleen contrast ratio (LSC10, LSC15 and LSC20) in group C (P>0.05), and differences between LSC10 and LSC15, LSC10 and LSC20, and LSC15 and LSC20 were also not statistically significant (P>0.05). The differences between the liver-to-spleen contrast ratio (LSC10, LSC15, and LSC20) in group D were statistically significant (P=0.034), but the pairwise comparison showed no significant differences between LSC10 and LSC15, LSC10 and LSC20, and LSC15 and LSC20 (P>0.05) (see *Figures 10*,*11*, *Table 7*).

Discussion

Gd-EOB-DTPA-enhanced MRI can increase the minute lesion detection rate compared with extracellular contrast agent-enhanced MRI and multi-slice spiral CT, which is mainly achieved by increasing the contrast of images in the hepatobiliary phase (23-26). The present study showed that all cases had improved in contrast evaluation indices after contrast agent injection compared with the plain scan, which is consistent with previously reported findings. Previous studies have also shown that the liver parenchyma would have better enhancement when the dose of Gd-EOB-DTPA have been increased (27-29). These findings are consistent with the result that the relative tissue enhancement of the hepatic parenchyma in each phase (LE10, 15 and 20) of the conventional-dose group (group D) was higher than that in the low-dose group (group C) in the prospective grouping study of different dose. At the same time, the relative tissue enhancement of the portal vein and splenic parenchyma in each phase (PE10, 15 and 20; SE10, 15 and 20) in the conventional-dose group were also higher than those in the low-dose group, which were also consistent with the previous studies (30,31) and this may be due to higher doses of Gd-EOB-DTPA in group D, with higher levels of residual contrast medium in the portal vein and splenic parenchyma at each point in time.

Besides these findings which were consistent with the previous studies, In the retrospective grouping study based on BMI values, the liver-to-portal vein contrast ratio of plain scan and hepatobiliary phase (LPC and LPC20) in group A were significantly higher than those in group B, but there was no obvious difference between the two groups in terms of the liver-to-spleen contrast ratio (LSC and LSC20). This may be related to the fact that the lava sequence used in this study was a fat suppression sequence and that the fat fraction of the liver and spleen was positively correlated with BMI (32-34). In the ratio of hepatic parenchymal signal to splenic parenchymal signal, BMI exerted a similar effect on the liver and spleen, i.e., the higher the BMI, the higher the liver and spleen fat

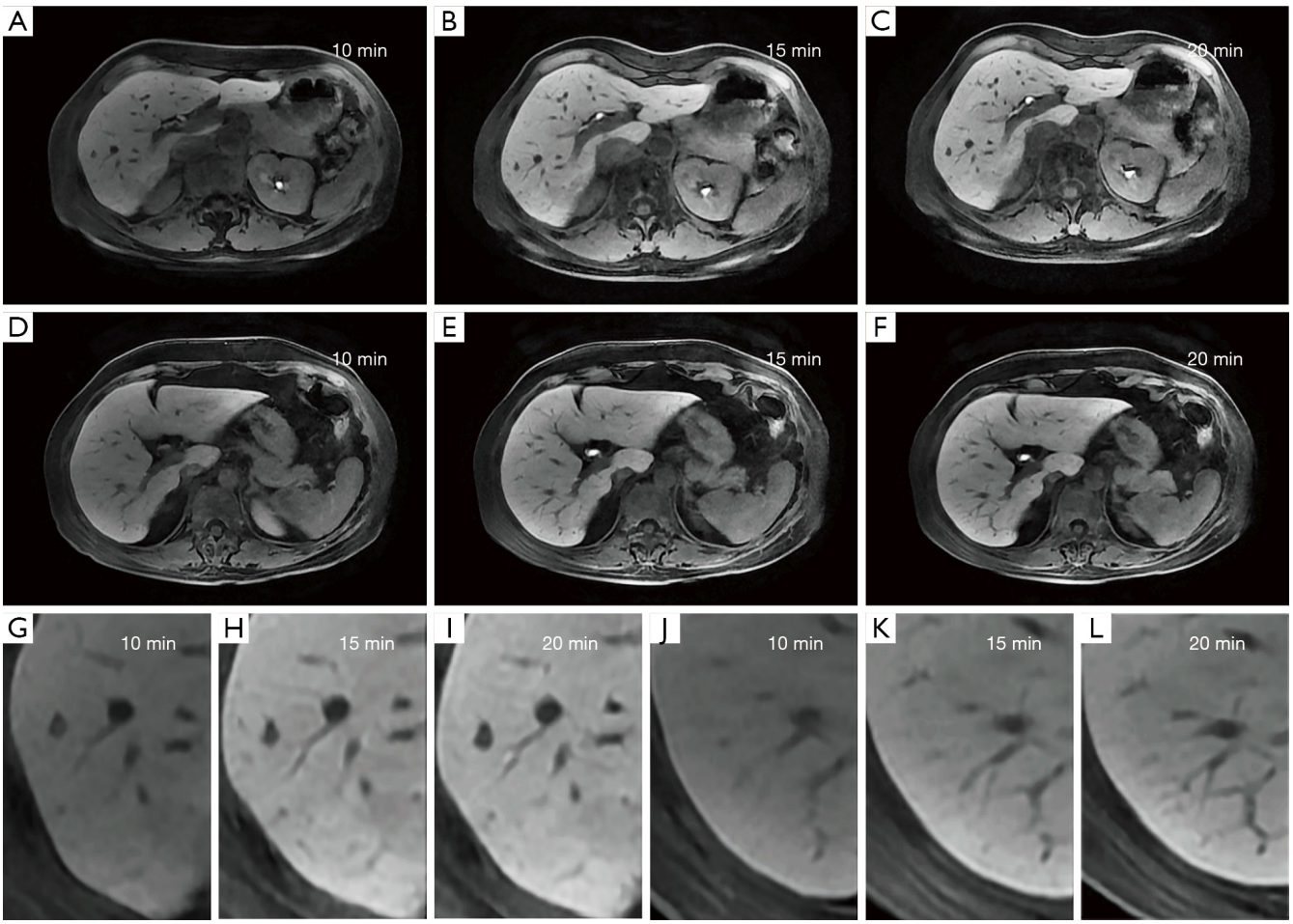

Figure 10 Prospective grouping study on different doses. (A,B,C,G,H,I) Different phase images of a patients with a BMI =20.32 kg/m^2 in group C, the liver-to-portal vein contrast ratio (LPC10, 15 and 20) and the liver-to-spleen contrast ratio (LSC10, 15 and 20) were 2.54, 2.79, 2.89, 1.17, 1.14 and 1.13, respectively. (D,E,FJ,K,L) Different phase images of a patients with a BMI =21.21 kg/m^2 in group D, the liver-to-portal vein contrast ratio (LPC10, 15 and 20) and the liver-to-spleen contrast ratio (LSC10, 15 and 20) were 2.09, 2.77, 2.81 1.07, 1.19, 1.20, respectively. BMI, body mass index; LSC10/15/20, ratio of hepatic parenchymal signal to splenic parenchymal signal in corresponding phases; LPC10/15/20, ratio of hepatic parenchymal signal to portal vein signal in corresponding phases.

fraction, which was manifested by both the liver and spleen producing more signal loss on the lava sequence, their ratio might be relatively constant, and there was no change in the two groups of patients with different BMIs. In terms of the ratio of hepatic parenchymal signal to portal vein signal, the effect of BMI on the liver and portal vein was different. For the portal vein signal, since the main component of the portal vein was flowing blood and was not affected by BMI, which was manifested by the portal vein signal remaining relatively stable on the lava sequence. However, for the hepatic parenchymal signal, group A with a lower BMI had lower liver fat content than the group B with a higher BMI, which was manifested by less hepatic parenchymal signal loss on the lava sequence in group A compared to group B (35). As a result, their ratio was significantly different between the two groups, and group A was higher than group B. In summary, the hepatobiliary phase image contrast in patients with a BMI <24 kg/m^2 was significantly higher than that in patients with a BMI ≥24 kg/m^2 using Gd-EOB-DTPA under the usual dose of administration, which was mainly manifested as a higher contrast between the hepatic parenchymal and hepatic blood vessels signals.

Considering that patients with a BMI <24 kg/m^2 had higher image contrast in the hepatobiliary phase in the

Table 6 Intergroup comparison of the indices in different dose groups

Index	Group C	Group D	*t*/*Z* value	P value
LE10	1.78±0.16	2.07±0.22	−4.201	<0.01
PE10	1.40±0.13	1.85±0.25	−6.226	<0.01
SE10	1.42±0.11	1.71±0.13	−6.614	<0.01
LE15	1.81 (1.78–1.97)	2.15 (2.06–2.44)	−3.754[1]	<0.01[1]
PE15	1.24±0.18	1.51±0.19	−3.955	<0.01
SE15	1.46±0.14	1.72±0.14	−5.182	<0.01
LE20	1.94±0.20	2.27±0.29	−3.655	<0.01
PE20	1.25±0.24	1.46±0.20	−2.539	0.017
SE20	1.48±0.14	1.71±0.15	−4.330	<0.01
LPC	1.73±0.16	1.73±0.18	−0.058	0.954
LSC	0.94±0.09	0.93±0.12	0.423	0.676
LPC10	2.19±0.18	1.94±0.17	4.001	<0.01
LSC10	1.17±0.09	1.11±0.12	1.527	0.138
LPC15	2.67±0.33	2.61±0.21	0.507	0.616
LSC15	1.22±0.13	1.22±0.13	0.099	0.922
LPC20	2.74±0.37	2.72±0.27	0.158	0.875
LSC20	1.24±0.12	1.23±0.13	0.213	0.833

[1], a significant difference at a P value <0.05 was observed using the Mann-Whitney *U* test. Indices were presented as mean ± standard deviation when the samples followed the normal distribution and median (lower quartile – upper quartile) when the samples did not follow the normal distribution. Group C: low-dose group; Group D: conventional-dose group. LE10/15/20, the relative tissue enhancement of liver, ratio of hepatic parenchymal signal in the corresponding phases to hepatic parenchymal signal in the plain scan; PE10/15/20, the relative tissue enhancement of portal vein, ratio of portal vein signal in the corresponding phases to portal vein signal in the plain scan; SE10/15/20, the relative tissue enhancement of spleen, ratio of splenic parenchymal signal in the corresponding phases to splenic parenchymal signal in the plain scan; LPC and LPC10/15/20, the contrast between liver and portal vein, ratio of hepatic parenchymal signal to portal vein signal in the plain scan and corresponding phases; LSC and LSC10/15/20, the contrast between liver and spleen, ratio of hepatic parenchymal signal to splenic parenchymal signal in the plain scan and corresponding phases.

retrospective grouping studies, this study further explored the feasibility of reducing the contrast medium doses in these patients (BMI <24 kg/m^2), while still obtaining good image contrast in the hepatobiliary phase. The results showed that the images of the low-dose group did not affect the issuance of diagnostic reports and the following phenomena were also observed between C and D groups in the image contrast comparison. Firstly, at the 10 min after administration phase, the liver-to-portal vein contrast ratio (LPC10) of group C was higher than that of group D, the difference in liver-to-spleen contrast ratio (LSC10) was not statistically significant, i.e., in this phase, group C was closer to the requirements of the 2018 LI-RADS CT/MRI manual for the contrast of hepatobiliary phase images and the high-contrast hepatobiliary phase of patients in group C had an earlier trend relative to that of group D. This may be due to the lower dose of contrast medium in group C. Meanwhile, the patients in both groups had no abnormalities in their liver and kidney functions, and the absorption and metabolism rates of the contrast agent were similar. At the same time point (10 min), patients in group C had less residual contrast medium in the hepatic blood vessels, including the portal vein, which made the relative tissue enhancement of portal vein in group C lower than group D, and then the liver-to-portal vein contrast ration (LPC10) was higher than that in group D. Secondly, in the 15 and 20 min after administration phases, there were no significant changes in the LPC15, LSC15, LPC20, and LSC20 in groups C and D. This showed that although the contrast medium dose used in group C was lower, there were no differences between the two groups in the image contrast of the 15 and 20 min phases after contrast injection. This result may be due to the lower contrast medium dose in group C decreasing the liver enhancement as well as reducing the residue of the contrast media in the portal vein and splenic parenchyma and then decreasing their intensification too, which might eventually keep these indices relatively stable. Thirdly. In the intragroup comparison of groups C and D, the LPC15 and LPC20 were higher than LPC10, indicating that the images contrast acquired by each group at 10 min were lower than that at 15 and 20 min after the injection, while the high-contrast hepatobiliary phase images still needed to wait for a longer time (15–20 min) even the half dose of Gd-EOB-DTPA were utilized. This result may be related to the fact that there was still more residue of the contrast agent in the hepatic blood vessels with such a short delay time (10 min). In summary, low-dose Gd-EOB-DTPA in patients with a BMI <24 kg/m^2 also yielded well-contrasted hepatobiliary phase images compared with the conventional doses, and the image contrast was even better than that in the conventional-dose group at 10 min after administration.

This study has limitations that should be noted. Firstly, bias was inevitable in the retrospective study section and

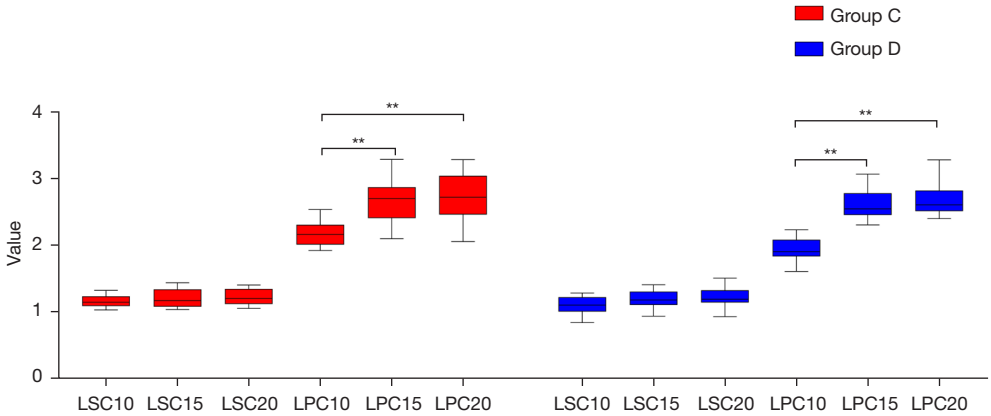

Figure 11 Intragroup comparison of the indices in different dose groups. **, P<0.01. Group C: low-dose group; Group D: conventional-dose group. LSC10/15/20, ratio of hepatic parenchymal signal to splenic parenchymal signal in corresponding phases; LPC10/15/20, ratio of hepatic parenchymal signal to portal vein signal in corresponding phases.

Table 7 Intragroup comparison of the indices in different dose groups

Delay time	Group C		Group D	
	LPC	LSC	LPC	LSC
10 min	2.19±0.18	1.17±0.09	1.94±0.17	1.11±0.12
15 min	2.67±0.33	1.22±0.13	2.61±0.21	1.22±0.13
20 min	2.74±0.37	1.24±0.12	2.72±0.27	1.23±0.13
F value	–	1.282	55.714	3.661
P value	<0.01[1]	0.288	<0.01	0.034
Multiple mean comparison	LPC15 > LPC10[2]; LPC20 > LPC10[2]	–	LPC15 > LPC10; LPC20 > LPC10	–

[1], the variance was uneven, so the Welch test was used; [2], the variance was uneven, so the Tamhane T2 method was used. Indices were presented as mean ± standard deviation. Group C: low-dose group; Group D: conventional-dose group. LPC, liver-to-portal vein contrast ratio; LSC, liver-to-spleen contrast ratio; LPC10/15/20, the contrast between liver and portal vein, ratio of hepatic parenchymal signal to portal vein signal in corresponding phases.

cases of liver function impairment were not included in both retrospective and prospective studies. Furthermore, the assessment of the hepatobiliary phase image contrast in this study was only based on the requirements of the 2018 LI-RADS CT/MRI manual and did not include specific lesion signal performance. In the future, further optimization of the dose of contrast medium for specific lesions and patients with liver function impairment according to the BMI is needed.

Conclusions

The hepatobiliary phase image contrast in patients with a BMI <24 kg/m^2 was higher than that in patients with a BMI ≥24 kg/m^2 at the conventional dose (0.025 mmol/kg), which was mainly manifested by a higher contrast between the hepatic parenchymal and portal vein signals. The application of low-dose (0.0125 mmol/kg) Gd-EOB-DTPA in patients with normal hepatic and renal function and a BMI <24 kg/m^2 can also produce good image contrast in the hepatobiliary phase at 15–20 min after contrast injection.

Acknowledgments

The participants are all sincerely appreciated by the authors for taking part in our study.
Funding: None.

Footnote

Reporting Checklist: The authors have completed the GRRAS reporting checklist. Available at https://qims.amegroups.com/article/view/10.21037/qims-23-653/rc

Conflicts of Interest: All authors have completed the ICMJE uniform disclosure form (available at https://qims.amegroups.com/article/view/10.21037/qims-23-653/coif). The authors have no conflicts of interest to declare.

Ethical Statement: The authors are accountable for all aspects of the work in ensuring that questions related to the accuracy or integrity of any part of the work are appropriately investigated and resolved. The study was conducted in accordance with the Declaration of Helsinki (as revised in 2013). The study was approved by the Ethics Committee of The First Affiliated Hospital of Chongqing Medical University and informed consent was taken from all the patients.

References

1. Vernuccio F, Bruno A, Costanzo V, Bartolotta TV, Vieni S, Midiri M, Salvaggio G, Brancatelli G. Comparison of the Enhancement Pattern of Hepatic Hemangioma on Magnetic Resonance Imaging Performed With Gd-EOB-DTPA Versus Gd-BOPTA. Curr Probl Diagn Radiol 2020;49:398-403.
2. Hayoz R, Vietti-Violi N, Duran R, Knebel JF, Ledoux JB, Dromain C. The combination of hepatobiliary phase with Gd-EOB-DTPA and DWI is highly accurate for the detection and characterization of liver metastases from neuroendocrine tumor. Eur Radiol 2020;30:6593-602.
3. Dai H, Lu M, Huang B, Tang M, Pang T, Liao B, Cai H, Huang M, Zhou Y, Chen X, Ding H, Feng ST. Considerable effects of imaging sequences, feature extraction, feature selection, and classifiers on radiomics-based prediction of microvascular invasion in hepatocellular carcinoma using magnetic resonance imaging. Quant Imaging Med Surg 2021;11:1836-53.
4. Vanhooymissen IJSML, Thomeer MG, Braun LMM, Gest B, van Koeverden S, Willemssen FE, Hunink M, De Man RA, Ijzermans JN, Dwarkasing RS. Intrapatient Comparison of the Hepatobiliary Phase of Gd-BOPTA and Gd-EOB-DTPA in the Differentiation of Hepatocellular Adenoma From Focal Nodular Hyperplasia. J Magn Reson Imaging 2019;49:700-10.
5. Wang F, Numata K, Okada M, Chuma M, Nihonmatsu H, Moriya S, Nozaki A, Ogushi K, Luo W, Ruan L, Nakano M, Otani M, Inayama Y, Maeda S. Comparison of Sonazoid contrast-enhanced ultrasound and gadolinium-ethoxybenzyl-diethylenetriamine pentaacetic acid MRI for the histological diagnosis of hepatocellular carcinoma. Quant Imaging Med Surg 2021;11:2521-40.
6. Park JH, Chung YE, Seo N, Choi JY, Park MS, Kim MJ. Hepatobiliary phase signal intensity: A potential method of diagnosing HCC with atypical imaging features among LR-M observations. PLoS One 2021;16:e0257308.
7. Wang X, Wang Y, Zhang Z, Zhou M, Zhou X, Zhao H, Xing J, Zhou Y. Rim enhancement on hepatobiliary phase of pre-treatment 3.0 T MRI: A potential marker for early chemotherapy response in colorectal liver metastases treated with XELOX. Eur J Radiol 2021;143:109887.
8. Hussain HK. Hepatobiliary-Phase Hypointense Nodules without Arterial Phase Hyperenhancement: Time to Act. Acad Radiol 2022;29:211-2.
9. Obmann VC, Catucci D, Berzigotti A, Gräni C, Ebner L, Heverhagen JT, Christe A, Huber AT. T1 reduction rate with Gd-EOB-DTPA determines liver function on both 1.5 T and 3 T MRI. Sci Rep 2022;12:4716.
10. Tamada T, Ito K, Yamamoto A, Yasokawa K, Higaki A, Kanki A, Sato T, Tanimoto D, Higashi H. Hypointense hepatocellular nodules on hepatobiliary phase of Gd-EOB-DTPA-enhanced MRI: can increasing the flip angle improve conspicuity of lesions? J Magn Reson Imaging 2013;37:1093-9.
11. Motosugi U, Ichikawa T, Sou H, Sano K, Tominaga L, Muhi A, Araki T. Distinguishing hypervascular pseudolesions of the liver from hypervascular hepatocellular carcinomas with gadoxetic acid-enhanced MR imaging. Radiology 2010;256:151-8.

12. Unal E, Idilman IS, Karçaaltıncaba M. Multiparametric or practical quantitative liver MRI: towards millisecond, fat fraction, kilopascal and function era. Expert Rev Gastroenterol Hepatol 2017;11:167-82.
13. Sollmann N, Bonnheim NB, Joseph GB, Chachad R, Zhou J, Akkaya Z, Pirmoazen AM, Bailey JF, Guo X, Lazar AA, Link TM, Fields AJ, Krug R. Paraspinal Muscle in Chronic Low Back Pain: Comparison Between Standard Parameters and Chemical Shift Encoding-Based Water-Fat MRI. J Magn Reson Imaging 2022;56:1600-8.
14. Gallagher D, Heymsfield SB, Heo M, Jebb SA, Murgatroyd PR, Sakamoto Y. Healthy percentage body fat ranges: an approach for developing guidelines based on body mass index. Am J Clin Nutr 2000;72:694-701.
15. Pacheco LS, Blanco E, Burrows R, Correa-Burrows P, Santos JL, Gahagan S. Eating behavior and body composition in Chilean young adults. Appetite 2021;156:104857.
16. Andreacchi AT, Griffith LE, Guindon GE, Mayhew A, Bassim C, Pigeyre M, Stranges S, Anderson LN. Body mass index, waist circumference, waist-to-hip ratio, and body fat in relation to health care use in the Canadian Longitudinal Study on Aging. Int J Obes (Lond) 2021;45:666-76.
17. Zhang Y, Cao Y, Shih GL, Hecht EM, Prince MR. Extent of signal hyperintensity on unenhanced T1-weighted brain MR images after more than 35 administrations of linear gadolinium-based contrast agents. Radiology 2017;282:516-25.
18. Gibson SE, Farver CF, Prayson RA. Multiorgan involvement in nephrogenic fibrosing dermopathy: an autopsy case and review of the literature. Arch Pathol Lab Med 2006;130:209-12.
19. Darrah TH, Prutsman-Pfeiffer JJ, Poreda RJ, Ellen Campbell M, Hauschka PV, Hannigan RE. Incorporation of excess gadolinium into human bone from medical contrast agents. Metallomics 2009;1:479-88.
20. Ramalho J, Semelka RC, Ramalho M, Nunes RH, AlObaidy M, Castillo M. Gadolinium-Based Contrast Agent Accumulation and Toxicity: An Update. AJNR Am J Neuroradiol 2016;37:1192-8.
21. Kanal E. Gadolinium based contrast agents (GBCA): Safety overview after 3 decades of clinical experience. Magn Reson Imaging 2016;34:1341-5.
22. Chen C, Lu FC; . The guidelines for prevention and control of overweight and obesity in Chinese adults. Biomed Environ Sci 2004;17 Suppl:1-36.
23. Vogl TJ, Kümmel S, Hammerstingl R, Schellenbeck M, Schumacher G, Balzer T, Schwarz W, Müller PK, Bechstein WO, Mack MG, Söllner O, Felix R. Liver tumors: comparison of MR imaging with Gd-EOB-DTPA and Gd-DTPA. Radiology 1996;200:59-67.
24. Böttcher J, Hansch A, Pfeil A, Schmidt P, Malich A, Schneeweiss A, Maurer MH, Streitparth F, Teichgräber UK, Renz DM. Detection and classification of different liver lesions: comparison of Gd-EOB-DTPA-enhanced MRI versus multiphasic spiral CT in a clinical single centre investigation. Eur J Radiol 2013;82:1860-9.
25. Poetter-Lang S, Dovjak GO, Messner A, Ambros R, Polanec SH, Baltzer PAT, Kristic A, Herold A, Hodge JC, Weber M, Bastati N, Ba-Ssalamah A. Influence of dilution on arterial-phase artifacts and signal intensity on gadoxetic acid-enhanced liver MRI. Eur Radiol 2023;33:523-34.
26. Zhang Y, Numata K, Du Y, Maeda S. Contrast Agents for Hepatocellular Carcinoma Imaging: Value and Progression. Front Oncol 2022;12:921667.
27. Stern W, Schick F, Kopp AF, Reimer P, Shamsi K, Claussen CD, Laniado M. Dynamic MR imaging of liver metastases with Gd-EOB-DTPA. Acta Radiol 2000;41:255-62.
28. Río Bártulos C, Senk K, Schumacher M, Plath J, Kaiser N, Bade R, Woetzel J, Wiggermann P. Assessment of liver function with MRI: where do we stand? Front Med (Lausanne) 2022;9:839919.
29. Aslan S, Eryuruk U, Tasdemir MN, Cakir IM. Determining the efficacy of functional liver imaging score (FLIS) obtained from gadoxetic acid-enhanced MRI in patients with chronic liver disease and liver cirrhosis: the relationship between Albumin-Bilirubin (ALBI) grade and FLIS. Abdom Radiol (NY) 2022;47:2325-34.
30. Motosugi U, Ichikawa T, Sano K, Sou H, Onohara K, Muhi A, Kitamura T, Amemiya F, Enomoto N, Matsuda M, Asakawa M, Fujii H, Araki T. Double-dose gadoxetic Acid-enhanced magnetic resonance imaging in patients with chronic liver disease. Invest Radiol 2011;46:141-5.
31. Rendell VR, Winslow ER, Colgan TJ, Kovacs SK, Mühler MR, Knobloch G, Loeffler AG, Agni RM, Reeder SB. Radiologic-pathologic correlation of lesions in resected liver specimens with an ex vivo MRI-compatible localization device. Eur Radiol 2023;33:535-44.
32. Rinella ME, Alonso E, Rao S, Whitington P, Fryer J, Abecassis M, Superina R, Flamm SL, Blei AT. Body mass index as a predictor of hepatic steatosis in living liver donors. Liver Transpl 2001;7:409-14.

33. Seraj SM, Al-Zaghal A, Zadeh MZ, Jahangiri P, Pournazari K, Raynor WY, Werner TJ, Høilund-Carlsen PF, Alavi A, Hunt SJ. Dynamics of fluorine-18-fluorodeoxyglucose uptake in the liver and its correlation with hepatic fat content and BMI. Nucl Med Commun 2019;40:545-51.
34. Sijens PE, Edens MA, Bakker SJ, Stolk RP. MRI-determined fat content of human liver, pancreas and kidney. World J Gastroenterol 2010;16:1993-8.
35. Steffen IG, Weissmann T, Rothe JH, Geisel D, Chopra SS, Kahn J, Hamm B, Denecke T. Does hepatic steatosis influence the detection rate of metastases in the hepatobiliary phase of gadoxetic acid-enhanced MRI? J Clin Med 2020;10:98.

Cite this article as: Chen R, Lu Y, Xiao Z, Zhang Z, Lv F, Lv F. Effect of body mass index (BMI) on image contrast in the hepatobiliary phase of Gd-EOB-DTPA-enhanced-MRI and the feasibility of the application of half-dose Gd-EOB-DTPA to hepatobiliary phase imaging in patients with a BMI less than 24: a comparative study. Quant Imaging Med Surg 2023;13(9):6176-6192. doi: 10.21037/qims-23-653

